Supplement of Atmos. Chem. Phys., 21, 6481–6508, 2021
https://doi.org/10.5194/acp-21-6481-2021-supplement

Atmospheric Chemistry and Physics
Open Access
EGU

Supplement of

Spatial and temporal variability in the hydroxyl (OH) radical: understanding the role of large-scale climate features and their influence on OH through its dynamical and photochemical drivers

Daniel C. Anderson et al.

Correspondence to: Daniel C. Anderson (daniel.c.anderson@nasa.gov)

Supplementary Information

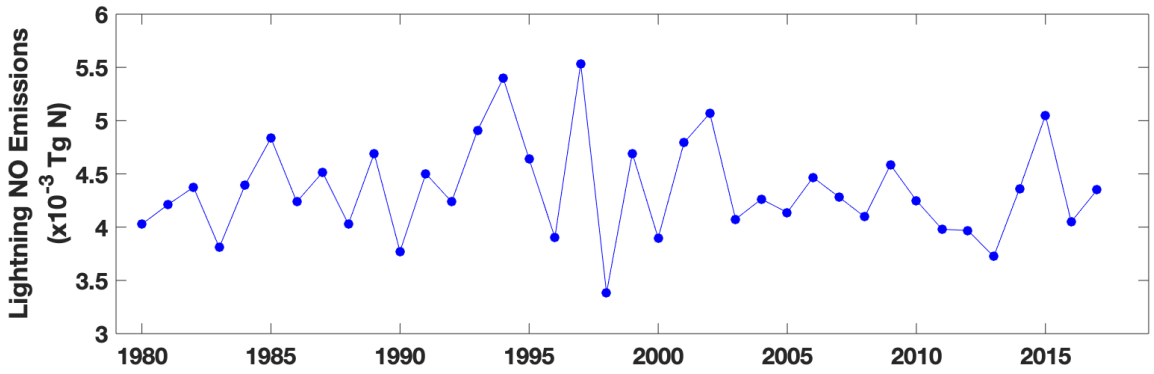

Figure S1: *Time series of total lightning NO emissions from M2GMI averaged over the region 15° S to 15° N and 150° to 250° E.*

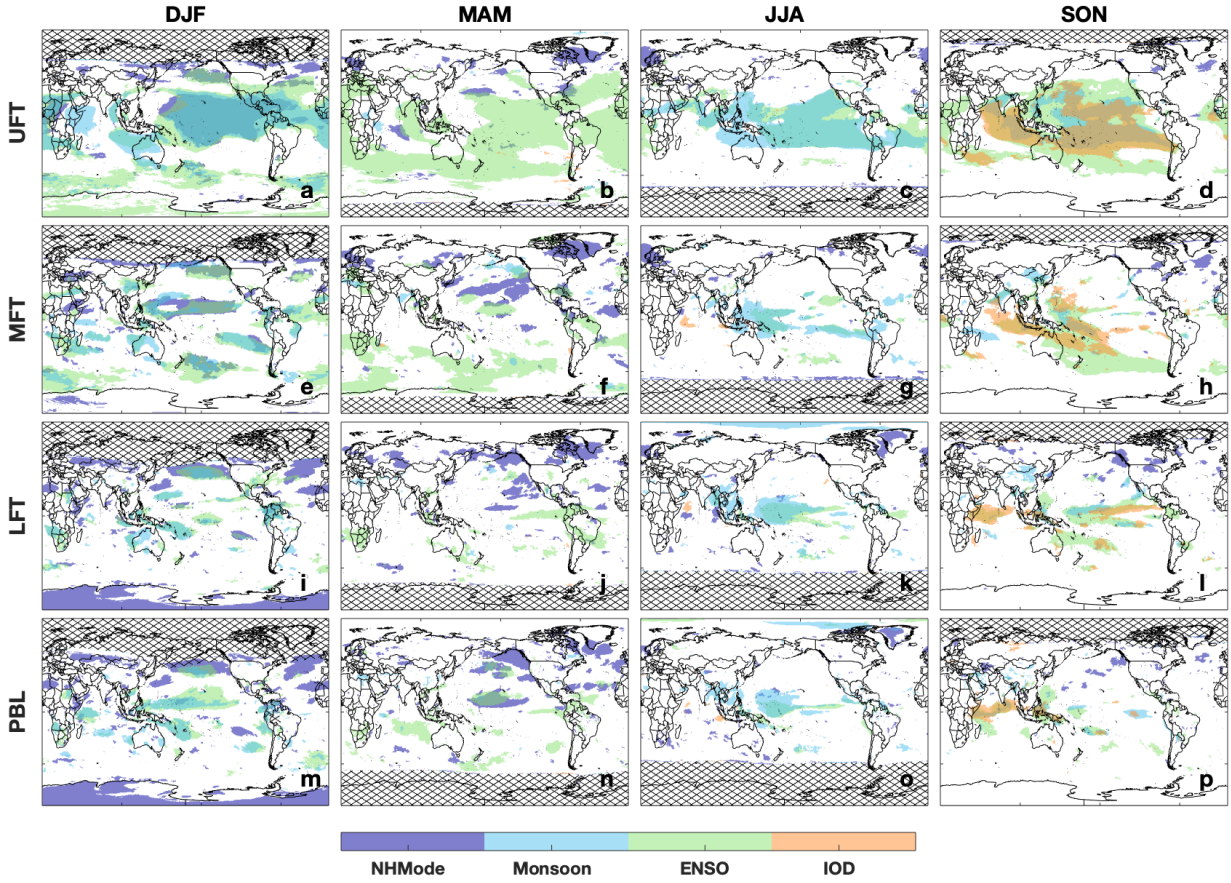

Figure S2: *Same as Figure 5 but for each layer.*

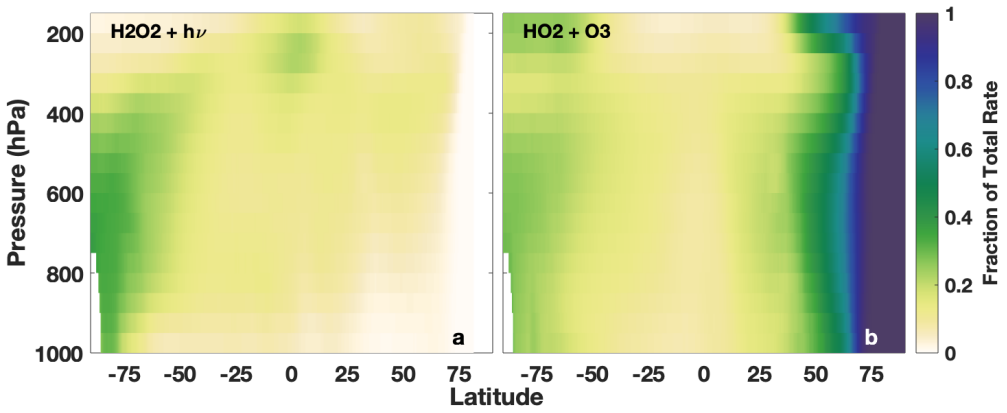

Figure S3: *Same as Figure 6, except for the H_2O_2 photolysis (a) and $HO_2 + O_3$ (b) reactions.*

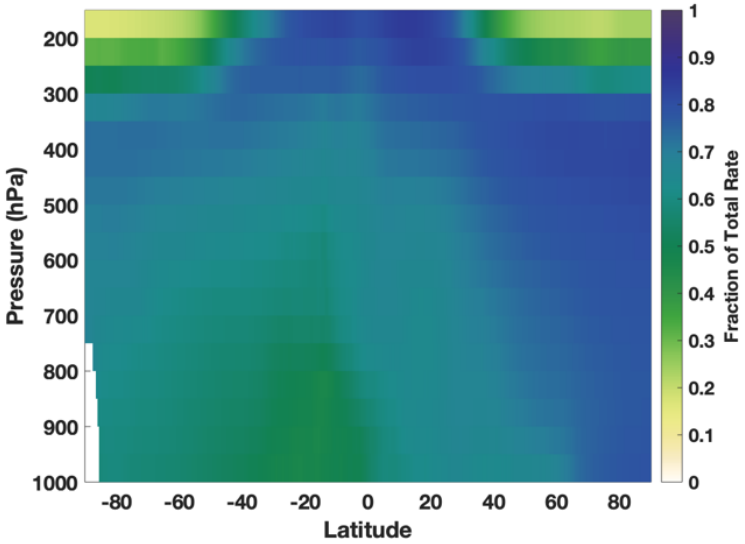

Figure S4: *Zonal mean of the fraction of the total OH loss rate attributable to the reaction of CO with OH.*

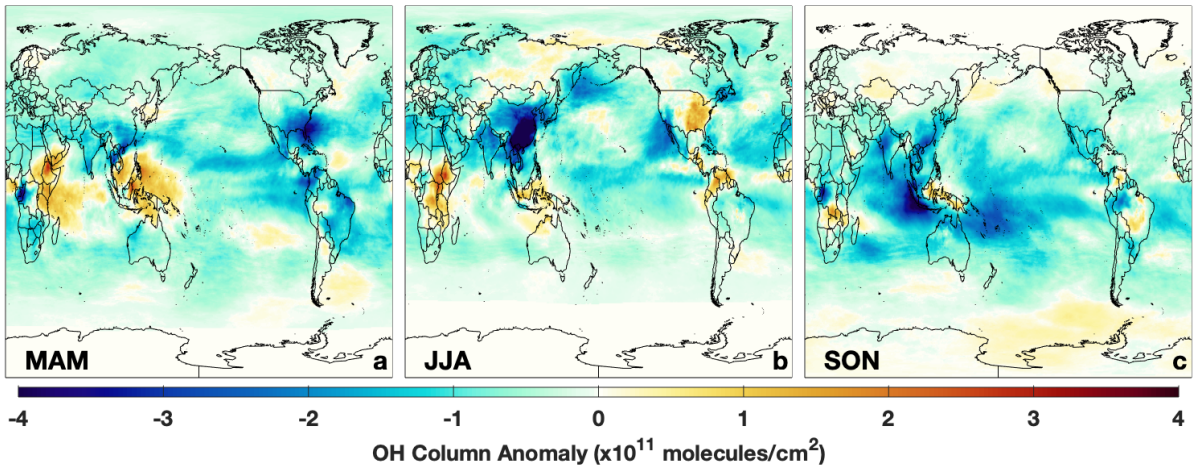

Figure S5: *Same as panel a of Figure 7 but for MAM (a), JJA (b), and SON (c).*

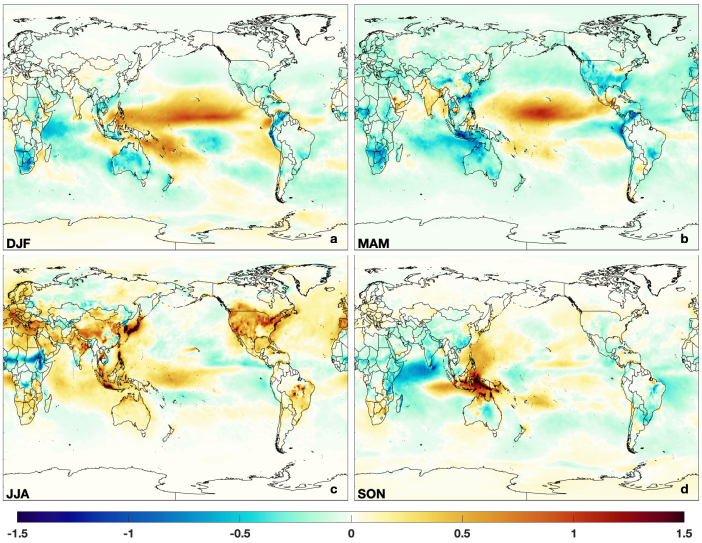

Figure S6: *The 2nd EOF of PBL OH from MERRA2 GMI for DJF (a), MAM (b), JJA (c), and SON (d)*

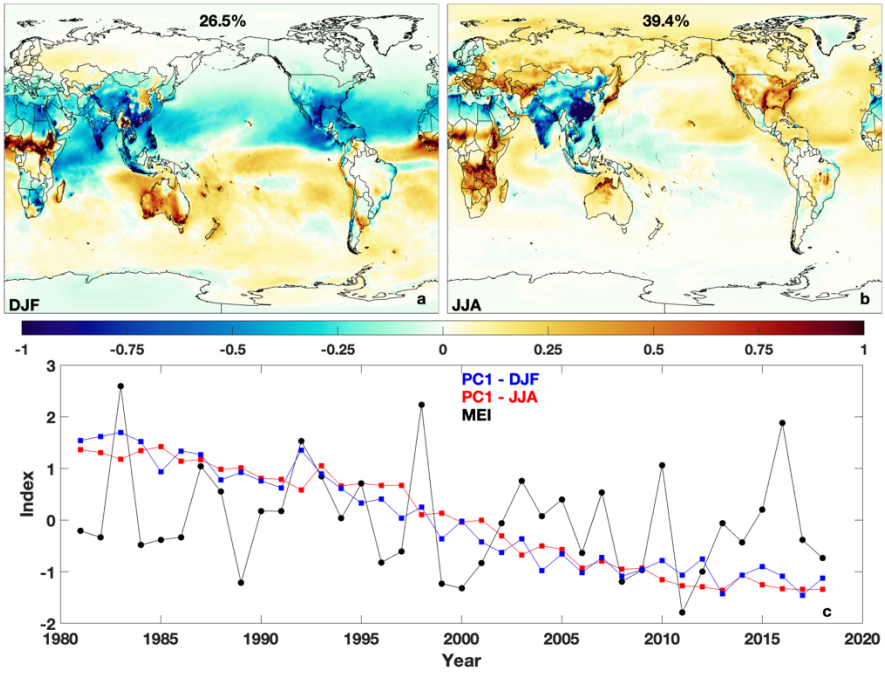

Figure S7: *First EOF of OH in the PBL level for DJF (a) and JJA (b). The contribution of the first EOF to the total variance is also indicated. The 1st Principal Component time series (c) is also shown for DJF (blue) and JJA (red) while the MEI is shown in black.*

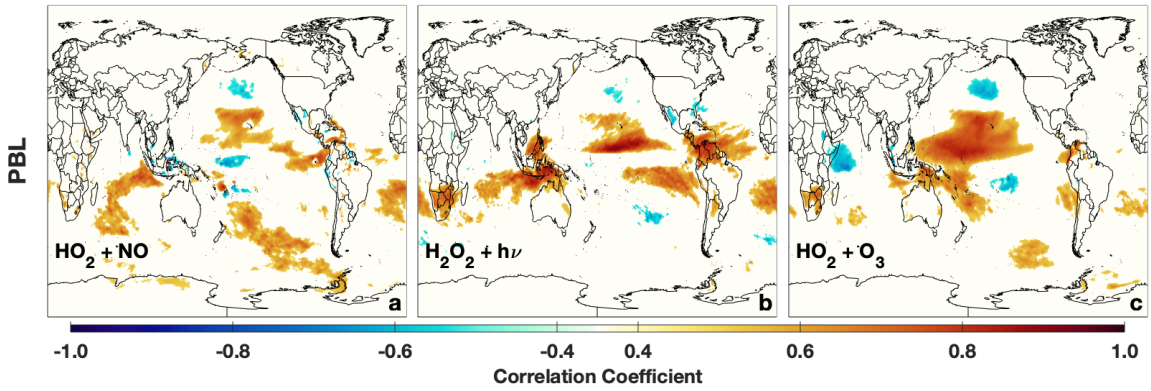

Figure S8: *Correlation of the indicated OH production reaction with the MEI for the PBL layer.*

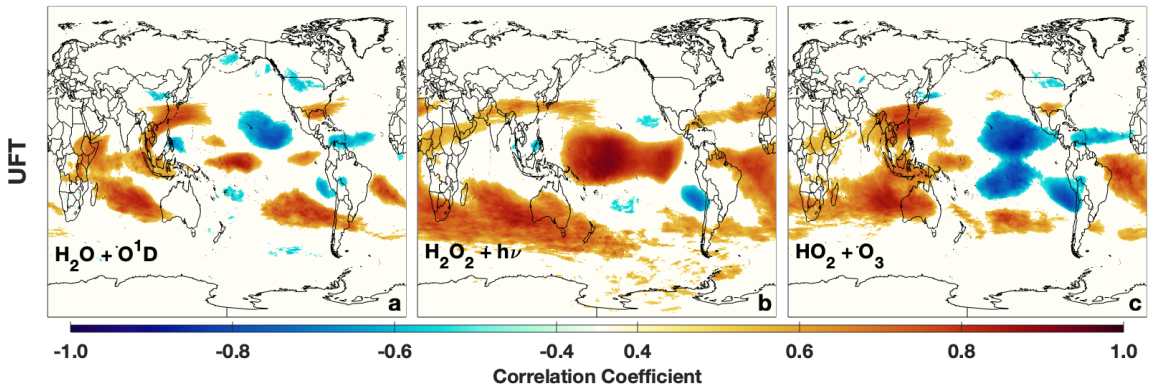

Figure S9: *Correlation of the indicated OH production reaction with the MEI for the UFT layer.*

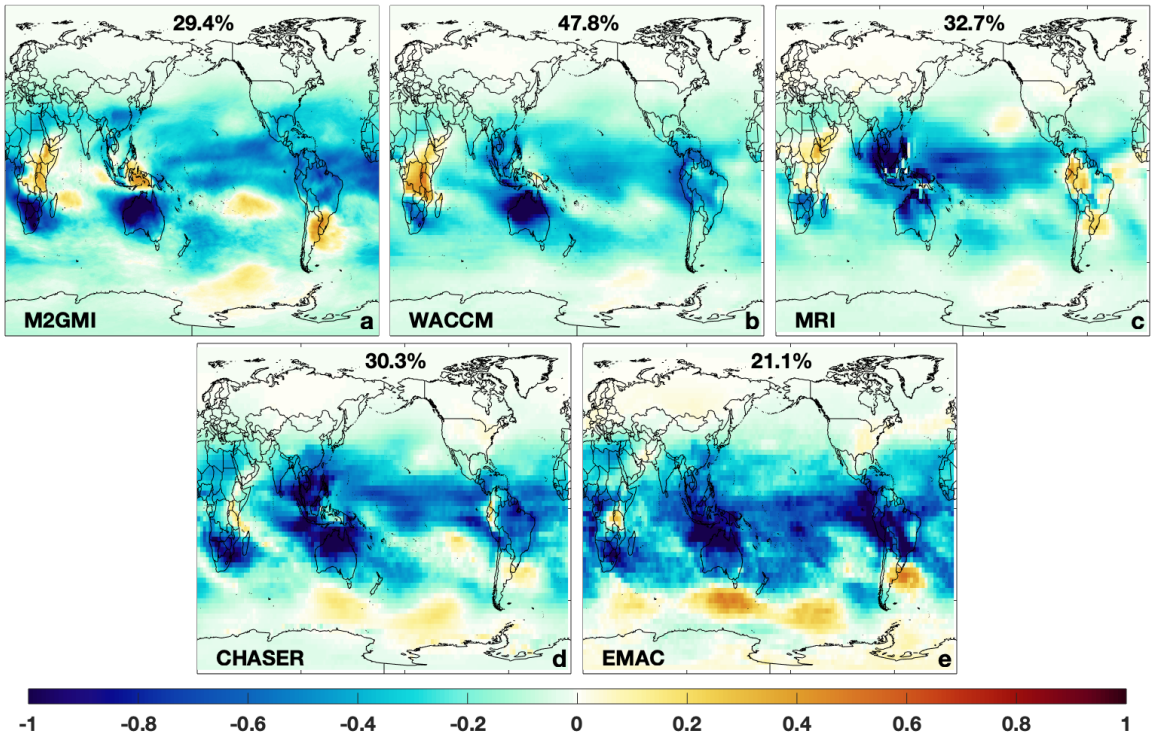

Figure S10: *First EOF of TCOH for M2GMI and the CCMI models evaluated here for DJF. The contribution of the first EOF to the total variance is also indicated.*

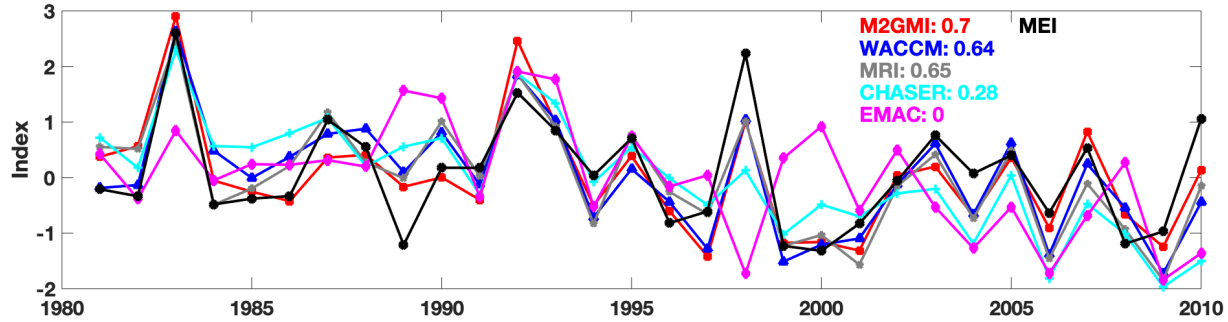

Figure S11: *Time series of the first EOF of TCOH for the models evaluated here for DJF as well as the MEI time series. The r^2 value of the correlation between the time series for the individual models and the MEI is also shown.*

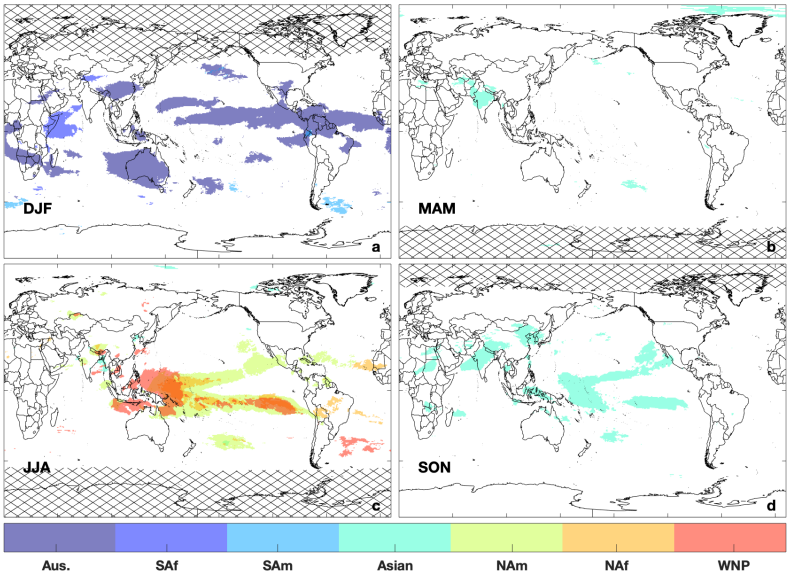

Figure S12: *For each season, regions that show a significant correlation (absolute value of r > 0.5) between TCOH and indices for the different monsoons: Australian (Aus.), South African (SAf), South American (Sam), Indian, North American (Nam), North African (NAf), and the Western North Pacific Monsoon (WNPM).*

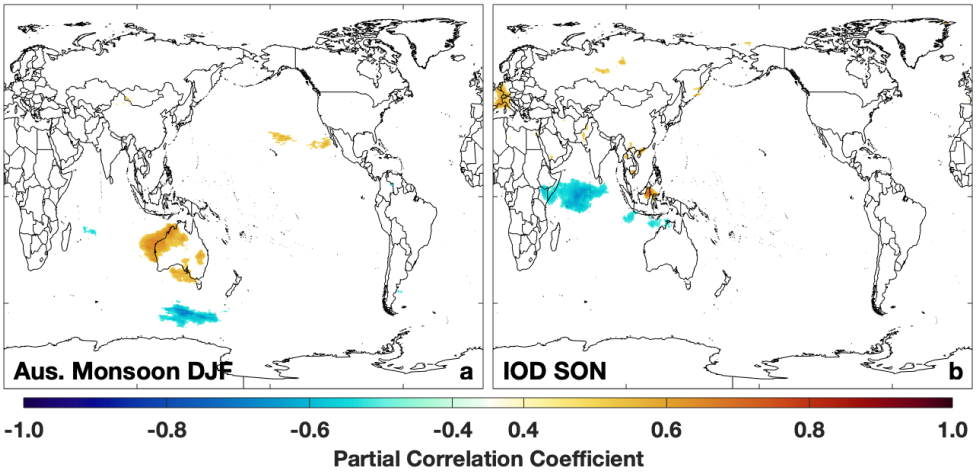

Figure S13: *Partial correlation of TCOH with the Australian monsoon (a) and IOD (b) during the indicated season taking into account the correlation of each with the MEI.*

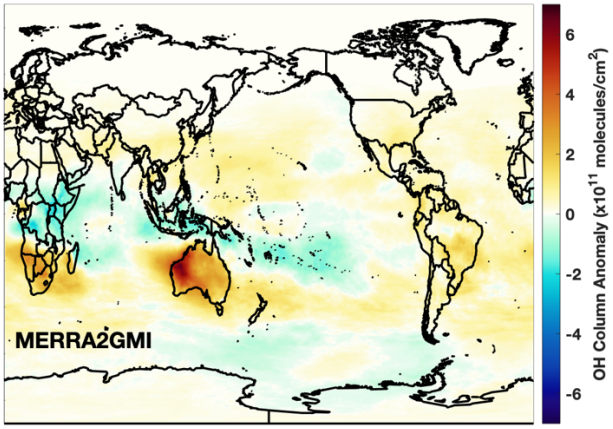

Figure S14: *Absolute difference in TCOH between years with an Australian monsoon index in the 75th percentile or higher and those years with a monsoon index between the 25th and 75th percentile.*

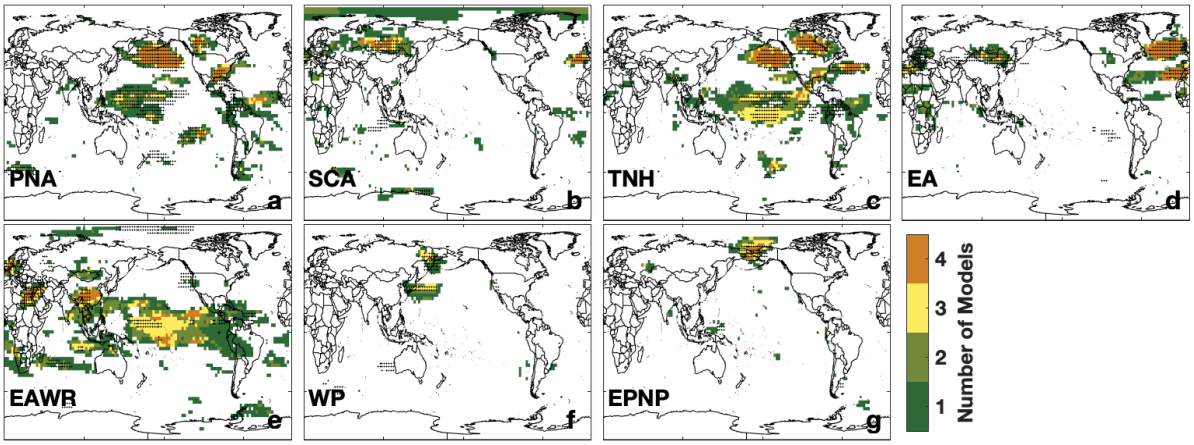

Figure S15: *Same as Figure 19 except for the PNA (a), the Scandinavian (b), Tropical Northern Hemisphere (c), East Atlantic (d), East Atlantic/Western Russian (e), West Pacific (f), and East Pacific/North Pacific (g) patterns during DJF.*

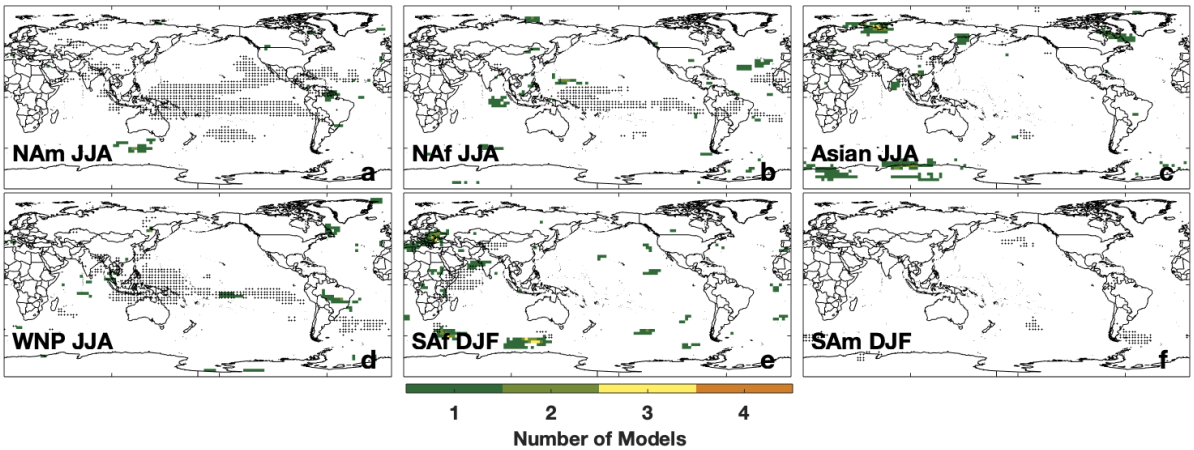

Figure S16: *Same as Figure 19 except for the North American (a), North African (b), Indian (c), Western North Pacific (d), South African (e), and South American (f) monsoons during the indicated season.*